SURFACE MORPHOLOGY OF SELECTIVE LASER-MELTED TITANIUM

H. Kyogoku*, Y. Shimizu*, and K. Yoshikawa†

*Faculty of Engineering, Kinki University, Higashihirosima, 739-2116 Japan
†NEXSYS, Wako, 351-0104 Japan

Abstract

The surface morphology of biomaterials is one of the most important biocompatibility factors. In this paper, the change in surface morphology of selective laser-melted titanium with process parameters was investigated to control the pore structure and mesh size. First, the process map which shows the relation between the morphology of laser-melted track and the process parameters such as laser power and scan speed was drawn by experiments. The laser-melted layer was fabricated on the basis of the process map. As a result, the surface morphology, especially pore structure and mesh size, of the layer is affected strongly by energy density as well as scan spacing.

Introduction

Selective laser meting (SLM) process has been widely utilized as one of the additive manufacturing (AM) processes in various industrial fields such as automotive, aerospace, biomaterials, and so on. In the field of biomaterials, especially, the surface morphology, such as porosity and pore size, is one of the most important factors for cell adhesion and proliferation [1]. Karageorgiou and Kaplan [1] reviewed the relationship between porosity and pore size of biomaterials used for bone regeneration, and recommended the fabrication of scaffolds with gradients in pore sizes using solid-free form technique. Recently, the research on the application of SLM and electron beam melting (EBM), that is easily able to control pore size, porosity and elastic modulus for fabricating biomaterials, of titanium and its alloy has been reported [2-4] because these provide a direct and reproducible process to fabricate biomaterials with controlled pore size, shape, and porosity [5]. Xue *et al*. [3] reported on the processing and biocompatibility evaluation of laser processed porous titanium by the LENS^{TM} method. They described that cells spread well on the surface of porous Ti and formed strong local adhesion, and a critical pore size of 200 μm or higher is needed for cell ingrowth into the pores. Haslauer *et al*. [4] reported on the biocompatibility of titanium alloy made using EBM process. They described that cellular proliferation on porous EBM disc was increased compared to discs made of commercial alloy, solid polished and unpolished EBM discs. Thus, the surface morphology of SLM and EBM processed Ti and its alloy is the most important factor for biomaterials.

The layer formation and surface morphology of SLM processed tool steel and stainless steel powders have been investigated. Niu and Chang [6-8] investigated on the effect of SLS processing parameters on the surface morphologies and microstructures, the mechanisms of liquid phase sintering, and the effect of the particle size and morphology on laser sinterability of high speed steel powder by using a SLS machine with a 25 W CO_2 laser. They reported on the mechanisms of formation of agglomerates and the effect of Marangoni flow in the melt pool on the morphology of the sintered tracks. Badrossamay and Childs [9, 10] investigated the effects of process parameters on the surface texture of tool steel and stainless steel powders, and the correlation between the laser melted surface and the parameters by using a research machine with a 240 W CO_2 laser. They reported that scan spacing and heat input affect strongly the surface morphology.

In this research, the change in surface morphology of SLM titanium with process parameters, such as laser power, scan speed and scan spacing, was investigated to control the pore structure and mesh size.

Experimental procedure

A laser sintering machine was used to fabricate specimens. The machine has a 50 W Yb-fiber laser (wave length:1090 nm), a galvanometer-scanner and a computer-controlled powder delivery and building system with chamber. The laser and galvanometer scanner are computer-controlled using the STL data converted from the CAD data. The spot size of laser beam is approximately 170μm.

In this research, a gas-atomized Ti powder was prepared. The mean particle diameter of the powder was 24.5 μm. The powder was filled into the container of powder supply unit and then laser-scanned at an atmosphere of argon gas under various fabrication conditions as follows;

- Laser power: 20~50 W
- Scan speed: 5~30 mm/s
- Scan spacing: 0.1~0.3 mm

The surface morphology and microstructure of the laser-scanned layers were examined by an optical microscope (OM) and a scanning electron microscope (SEM) with EDX.

Results and discussions

Fabrication conditions

(1) Change in morphology of single-track with laser power and scan speed

In order to fabricate sound laser scanned body, it is very important to examine the fabrication conditions, especially, laser power, scan speed, scan spacing and layer thickness are significant factors. The morphology of a track changes greatly with these factors. Figure 1 shows the change in morphology of a single-track with laser power and scan speed. The morphology of a single-track can be roughly classified into three types as follows:

(a) a smoothly continuous track
(b) a melted and balled continuous track
(c) a partially melted (balled) track

The difference in morphology of a track depends on not only energy density related to laser power and scan speed, but also the state of Marangoni flow and the oxygen content of molten pool, as already reported by Niu and Chang[6-8]. Therefore, the type (a) of smoothly continuous track is formed in the optimum energy density, and the type (b) or (c) of the track is formed in the case of higher energy density, in which creates “balling state”, or lower energy density, respectively.

In this research, the process map shown the effect of laser power and scan speed on the morphology of the track was drawn as shown in Fig.1. The value of energy density, *E*, calculated by the following equation was also given in this figure;

$$E = \frac{P}{v\ d}\,[\mathrm{J/mm^2}] \qquad (1)$$

where *P*=laser power [W], *v*=scan speed [mm/s], and *d*=laser spot size [mm].

It is found from this process map that a smoothly continuous track is not able to be formed at a scan-speed of more than 20 mm/s, that is, at an energy density of less than 15 J/mm^2.

A smoothly continuous track can be formed at a laser power of 30 W and 40 W. At a laser power of 20 W, especially a smooth surface track is formed, and the width of a track increases with increasing energy density. Thus it was found that a smoothly continuous track can be formed at a laser power between 30 and 40 W, at a scan speed between 5 and 10 mm/s, and at an energy density between 20 and 50 J/ mm^2.

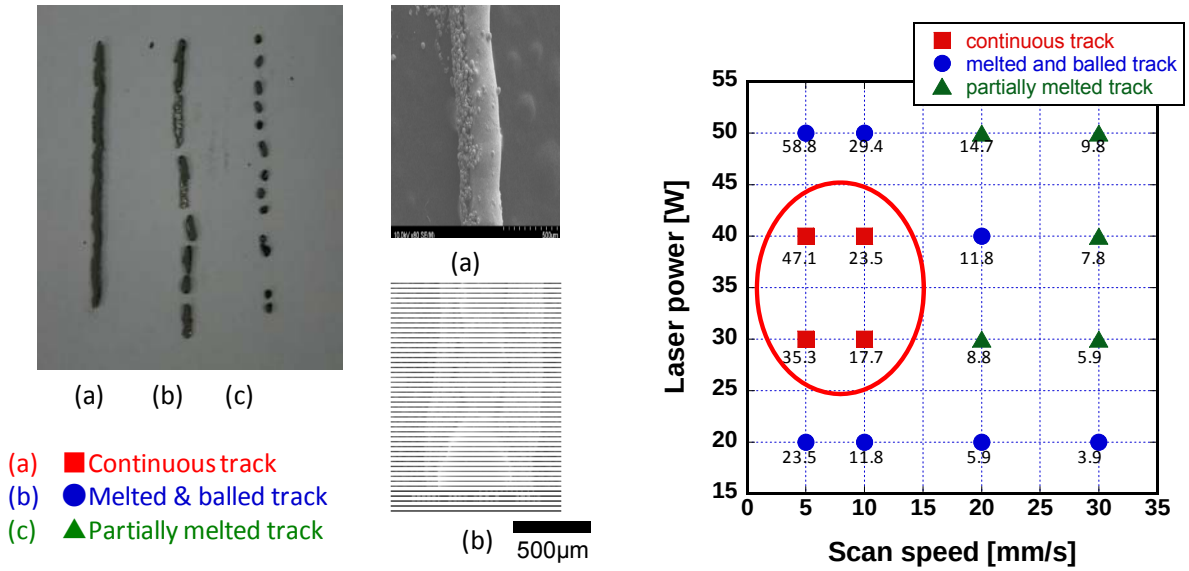

Fig.1 Effect of laser power and scan speed on the morphology of track

(2) Effect of energy density on the width of track

The change in surface morphology of the layer with scan spacing was examined. On the basis of the result of Fig.1, the laser power and the scan speed were changed at 20 ~50 W and 5~10 mm/s, respectively. The scan spacing was selected as 1/3 overlap of the spot size.

Figure 2 shows the variation in the width of track as a function of energy density. The width of track increases with increasing energy density, but it is approximately 450 μm at an energy density between 10 and 40 J/mm^2. The width of track is 300μm at an energy density of less than 10 J/mm^2 and it is 530μm at 47 J/mm^2. As a result, the fabrication condition of smoothly continuous track was as follows: at a laser power of 30 W and 40 W and at a scan speed of 5 mm/s and 10 mm/s.

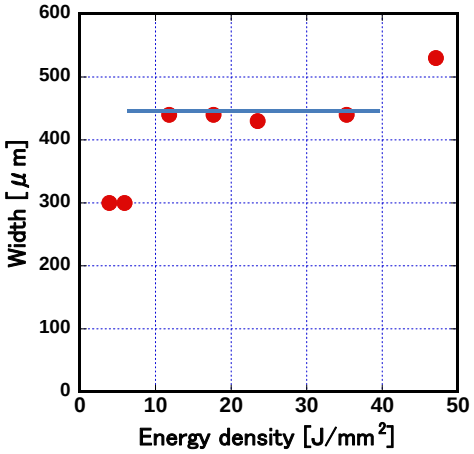

Fig.2 Variation in the width of track as a function of energy density

Surface morphology of laser-scanned layer

Figures 4 and 5 show the change in the surface morphology of the layer with laser power at a scan speed of 5 mm/s and 10 mm/s, respectively. A shown in Fig.4, in the case of the scan speed of 5 mm/s, the formation of agglomerates with lots of isolated pores are observed at 20 W, and the formation of columnar agglomerates parallel to the scan direction and prolonged pores are done at 30 W. The pore size of the layer laser-scanned at 20 W is 200~400 μm in average diameter. And the groove size of the columnar agglomerates formed at 30 W is around 200 μm in width. A relatively smooth surface without any pores is observed at 40 W and 50 W, but the undulation perpendicular to the scan direction is formed in the surface. On the other hand, as shown in Fig.5, in the case of the scan speed of 10 mm/s, the formation of columnar agglomerates parallel to the scan direction and isolated pores are observed at 20 W. A relatively smooth surface without any pores is observed at 30 W and 40 W, but the undulation perpendicular to the scan direction is formed in the surface. The smooth surface with less undulation is observed at 50 W. Thus the smooth surface is formed at a higher scan speed. This may be because the processing at a high speed with a relative low heat input and smaller heat affected zone gives less agglomeration [8].

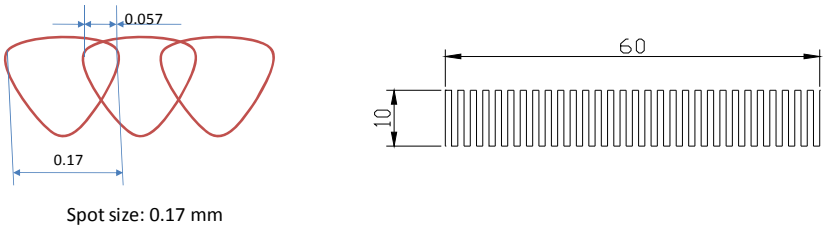

(a) Scan spacing (b) Laser scanning pattern

Fig.3 Laser scanning pattern and scan spacing

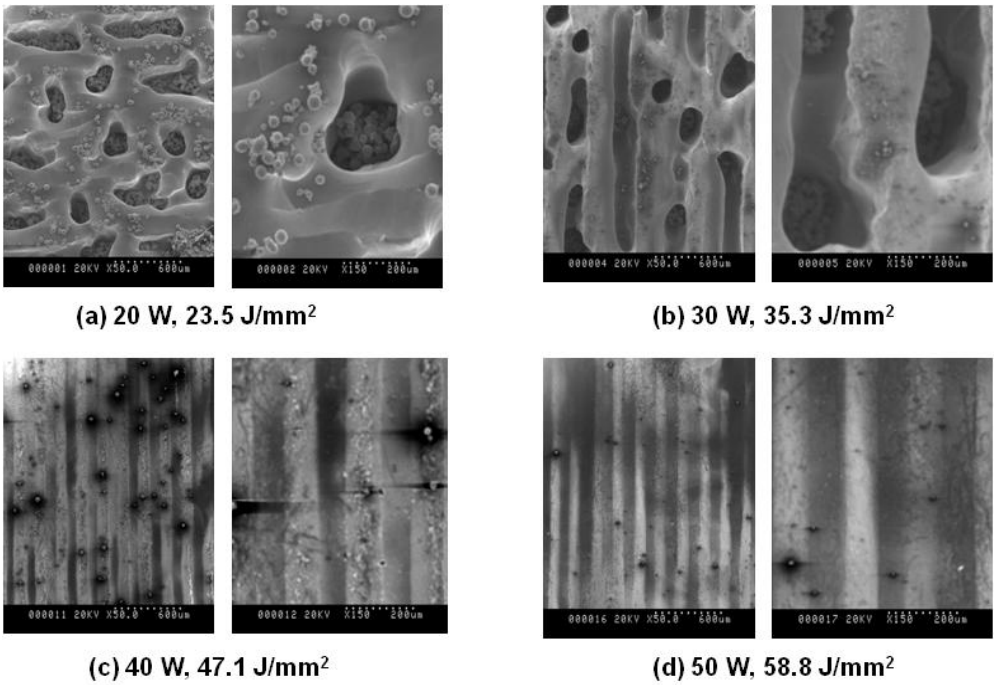

(a) 20 W, 23.5 J/mm^2 (b) 30 W, 35.3 J/mm^2

(c) 40 W, 47.1 J/mm^2 (d) 50 W, 58.8 J/mm^2

Fig.4 Change in surface morphology with laser power (scan speed: 5mm/s, scan pitch: 0.057mm)

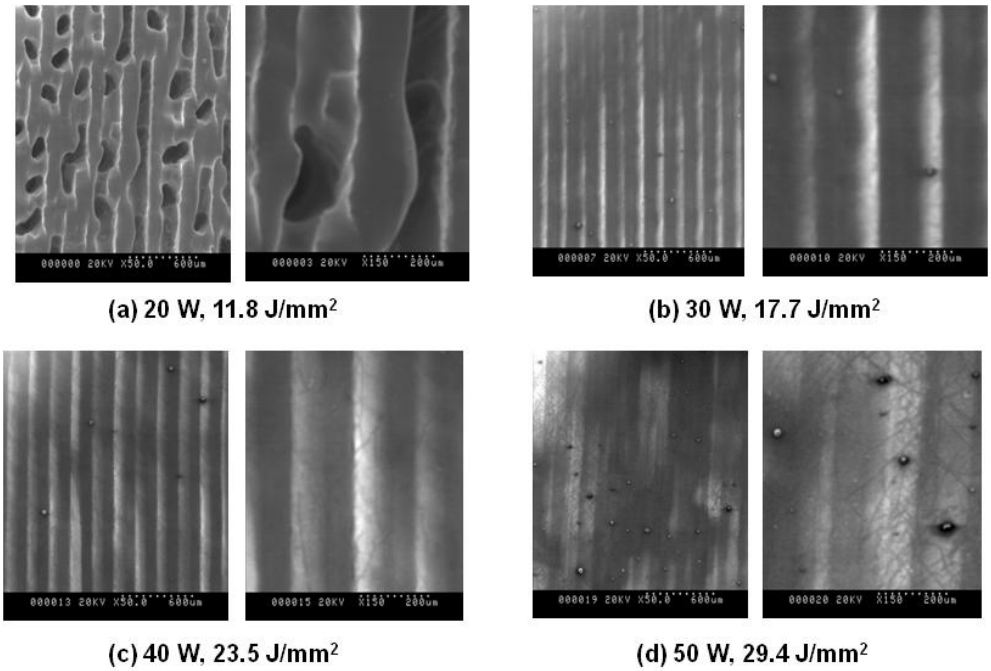

Fig.5 Change in surface morphology with laser power (scan speed: 10mm/s, scan pitch: 0.057mm)

In the case of the scan speed of 5 mm/s, the pore size in diameter is around 300 μm at 20 W, and the pore size in diameter or in width is around 200μm at 30 W. On the other hand, in the case of the scan speed of 10 mm/s, the pore size in diameter or in width is 100~200μm at 20 W. The minimum requirement for pore size is considered to be ~100 μm due to cell size, migration requirements and transport [1]. Teixeira *et al.* [11] suggested that porous Ti surfaces with pore sizes near 60 μm yield higher expression of osteoblast phenotype. Comparing with the results of these reports, the pore size of the surface laser-scanned is too large to yield higher expression of osteoblast. And also, the porosity is lower for cell adhesion and proliferation.

Thus the surface morphology of laser-scanned layer is unsuitable for expression of osteoblast. Therefore, the change in mesh spacing with scan spacing examined.

Effect of laser scanning conditions and scan-spacing

The change in mesh spacing with scan spacing was examined by changing the laser power at a scan speed of 5 mm/s and 10 mm/s. The OM micrograph of the mesh laser-scanned at 20 W is given in Fig.6. The SEM micrograph of the mesh laser-scanned at 20 W and 40 W is also given in Fig.7. The space of mesh is impossible to be clearly observed at a scan pitch of 1 mm, but is possible to be observed at a scan pitch of more than 1.5 mm.

In Fig.7, both of the melted part (A) and the sintered part (B) are observed. In the case of Fig.7 (a) of 20 W, the mesh spacing is around 600 μm, the width of melted part is around 300 μm as shown in Fig.2, and the width of sintered part is around 600 μm. Since the mesh spacing is too large for cell adhesion and proliferation, this mesh is unsuitable for scaffolds. In the case of Fig.7 (b) and (c) of 40 W, the mesh spacing is impossible to be clearly observed, but the melted part and the sintered part are observed. An example of the result of porous titanium fabricated by salt-leaching before pulse-current sintering is given in Fig.8. Osteogenic cells derived from human alveolar bone cultured on the specimen for 2 days highly adhere and proliferate in the sintered

part indicated by the arrow C. Therefore, in the case of the laser-scanned mesh, cells are possible to adhere and proliferate because of the mesh with a sintered part.

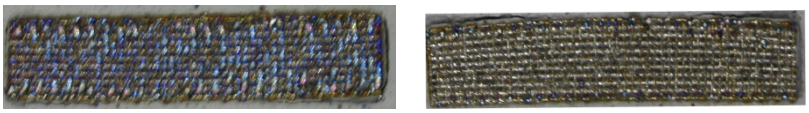

(a) Scan spacing: 1mm (b) Scan spacing: 1.5mm

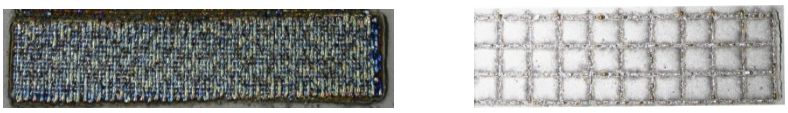

(c) Scan spacing: 2.5mm (d) Scan spacing: 5mm

Fig.6 OM micrographs of laser-scanned mesh (Laser power: 20 W, Scan speed:10 mm/s)

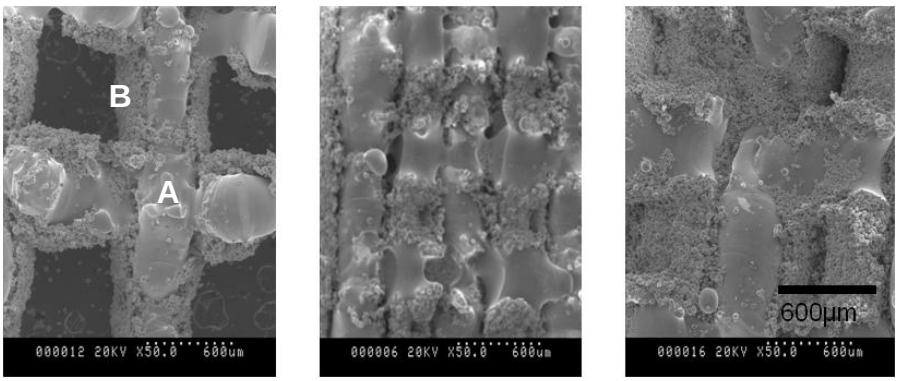

(a) Laser power 20 W (b) Laser power 40 W (c) Laser power 40 W
Scan speed 10 mm/s Scan speed 10 mm/s Scan speed 10 mm/s
Scan spacing 1.5 mm Scan spacing 1.0 mm Scan spacing 1.5 mm

Fig.7 SEM micrographs of laser-scanned mesh

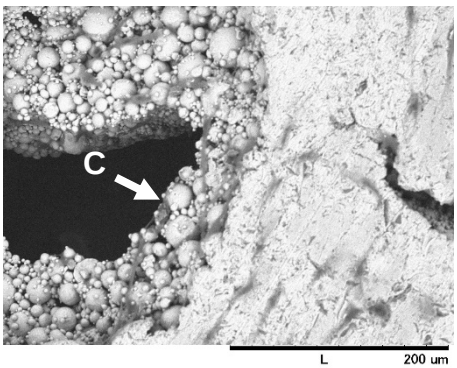

Fig.8 SEM micrograph of osteogenic cells derived from human alveolar bone cultured on sintered porous Ti for 2 days.

Conclusions

In this research, the change in surface morphology of SLM titanium with process parameters, such as laser power, scan speed and scan spacing, was investigated to control the pore structure and mesh size. The results obtained are as follows;

(1) The optimum fabrication condition of a smoothly continuous track was found out by drawing the process map which shows the relation between the morphology of laser-melted track and the process parameters such as laser power and scan speed.
(2) The laser-melted layer was fabricated on the basis of the process map. As a result, the surface morphology, especially pore structure and mesh size, of the layer is affected strongly by energy density as well as scan spacing.
(3) The surface morphology of laser-scanned layer is unsuitable for expression of osteoblast because of larger pores and lower porosity, but the laser-scanned mesh is possible to be suitable for cell adhesion and proliferation because of the mesh with a sintered part.

Acknowledgements

The authors would like to thank Professor Ishihata of Tohoku University for experimental support of this research. This work was supported by JSPS KAKENHI Grant Number 23560108.

References

[1] V. Kanageorgiou and D. Kaplan, “Porosity of 3D biomaterial scaffolds and osteogenesis”, Biomaterials, Vol. 26, (2005), pp.5474-5491.
[2] W. Traini, et al.., “Direct Laser Metal Sintering as a New Approach to Fabrication of an Isoelastic Functionally Graded Material for Manufacture of Porous Titanium Dental Implants”, Dental Materials, Vol.24, (2008), pp.1525-1533.
[3] W. Xue, B. W. Krishna, A. Bandyopadhyay, and S. Bose, “Processing and biocompatibility evaluation of laser processed porous titanium”, Acta Biomaterialia, Vol.3, (2007), pp.1007-1018.
[4] C. M. Haslauer, J. C. Springer, O. L.A. Harrysson, E. G. Loboa, N. A. Monterio-Riviere, and D. J. Marcellin-Little, “In vitro biocompatibility of titanium alloy discs made using direct metal fabrication”, Medical Engineering & Physics, Vol.32, (2010), pp.645-652.
[5] C. Gomez, B. Starly, A. Shokoufandeh, and W. Sun, “Transferring unit cell based tissue scaffold design to solid freefrom fabrication”, *Proceedings of Solid Freeform Fabrication Symposium 2006*, Austin, TX, (2006), pp.171-182.
[6] H.J. Niu and I.T.H. Chang, “Liquid phase sintering of M3/” high speed steel by selective laser sintering”, Scripta Materialia, Vol. 39, No. 1, (1998), pp.67–72.
[7] H.J. Niu and I.T.H. Chang, “Selective laser sintering of gas and water atomized high speed steel powders”, Scripta Materialia, Vol. 41, No. 1, (1999), pp.25–30.
[8] H.J. Niu and I.T.H. Chang, “Instability of scan tracks of selective laser sintering of high speed steel powder”, Scripta Materialia, Vol. 41, No. 11, (1999), pp.1229–1234.
[9] M. Badrossamay and T.H.C. Childs, “Further studies in selective laser melting of stainless and tool steel powders”, Int. Journal of Machine Tools & Manufacture, Vol.47, (2007), pp.779-784.
[10] M. Badrossamay and T.H.C. Childs, “Layer formation studies in selective laser melting of steel powders”, *Proceedings of Solid Freeform Fabrication Symposium 2006*, Austin, TX, (2006), pp.268-279.
[11] L.N. Teixeira, et al. “The influence of pore size on osteoblast phenotype expression in cultures grown on porous titanium”, Int. J. Oral & Maxillofacial Surgery, Vol.41, (2012), pp.1097-1101.